JACS
JOURNAL OF THE AMERICAN CHEMICAL SOCIETY
Communication
pubs.acs.org/JACS

Molecular Mechanism of Polyacrylate Helix Sense Switching across Its Free Energy Landscape

Adriana Pietropaolo*,† and Tamaki Nakano*,‡

†Dipartimento di Scienze della Salute, Università di Catanzaro, Viale Europa, 88100 Catanzaro, Italy
‡Catalysis Research Center (CRC), Hokkaido University, N 21, W 10, Kita-ku, Sapporo 001-0021, Japan

Supporting Information

ABSTRACT: Helical polymers with switchable screw sense are versatile frameworks for chiral functional materials. In this work, we reconstructed the free energy landscape of helical poly(2,7-bis(4-*tert*-butylphenyl)-fluoren-9-yl acrylate) [poly(BBPFA)], as its racemization is selectively driven by light without any rearrangement of chemical bonds. The chirality inversion was enforced by atomistic free energy simulations using chirality indices as reaction coordinates. The free energy landscape reproduced the experimental electronic circular dichroism spectra. We propose that the chirality inversion of poly(BBPFA) proceeds from a left-handed 3_1 helix via multistate free energy pathways to reach the right-handed 3_1 helix. The inversion is triggered by the rotation of biphenyl units with an activation barrier of 38 kcal/mol. To the best of our knowledge, this is the first report on the chiral inversion mechanism of a helical polymer determined in a quantitative way in the framework of atomistic free energy simulations.

Stereomutation of natural[1] and synthetic polymers[2] significantly affects their functions and properties.[3] For instance, chirality selection in proteins and chain folding are subtle events from the viewpoint of free energy that govern the global supramolecular shape.[4] A class of artificial polymers undergo a helix−helix transition.[3] Such polymers revert their helix sense through external stimuli,[5,6] showing a broad range of applications.[7−11] Helical polymer stereomutation is triggered mainly by chemical or thermal stimuli,[6] and a few examples of stereomutation triggered by light are known.[5] Most mutations by light involve the isomerization of a double bond[12] or rupture and formation of a chemical bond.[13]

Recently, a vinyl polymer bearing a fluorene-based side chain, poly(2,7-bis(4-*tert*-butylphenyl)fluoren-9-yl acrylate) [poly(BBPFA)] (Chart 1), was reported as the first polymer to undergo photoinduced racemization of a preferred-handed helix without any rearrangement of chemical bonds.[14] The polymer is stable against heat but is sensitive to light.[14] We postulated that light stimulation induces a biphenyl rearrangement that triggers the stereomutation.[14,15]

Chart 1. Schematic Representation of Helical poly(BBPFA)

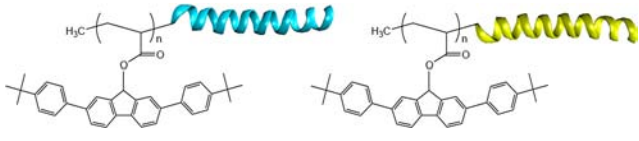

While a wealth of efforts and milestones have been provided for protein folding[16,17] and foldamers,[18,19] fewer contributions have been reported for stereomutation of synthetic helical polymers.[20] Pioneering contributions of polymer simulations based on coarse-grained,[21] two-state Ising models and force-field potentials for polyisocyanates[20d] have been provided. To date, however, detailed insights into the helix-reversal mechanism have not been disclosed in a quantitative manner through straightforward estimates of free energy pathways. Combining atomistic simulations with free energy methods[22,23] allows a direct quantitative estimate of energetics and structure. Recently, a chirality index[24,25] designed for biopolymers[26] and later introduced[27] into the more general path-collective variable[28] of the metadynamics algorithm[29] was proposed in order to quantify and discriminate helix handedness along the macromolecular chain. Its peculiarity is that it displays high sensitivity toward the helix sense without the typical artifacts due to the degeneracy introduced by using periodic angular descriptors.[27]

In this study, we performed well-tempered metadynamics[30] simulations for poly(BBPFA) in which chirality indices were used as reaction coordinates and to evaluate the structural characteristics. Moreover, to validate the accuracy of the free energy landscape, we calculated electronic circular dichroism (ECD) spectra using time-dependent density functional theory (TDDFT) with Becke's half-and-half (BH&HLYP) pseudopotential[31] for the bis(2,7-*tert*-butylphenyl)fluorenol ethyl ester monomeric unit and ZINDO[32] for isotactic right- and left-handed hexamer basins [see section 1.5 in the Supporting Information (SI) for polymer tacticity] and compared them to the experimental ECD spectra.

In particular, the s_G reaction coordinate identifies the path progress, indicating the handedness of a given conformation sampled during the simulation along the path connecting a 100% right-handed helix with a 100% left-handed helix. The z_G coordinate gives the distance from the endowed path, indicating how far a given conformation sampled during the simulation is from the path connecting the 100% right-handed and 100% left-handed helixes. Thus, s_G deals with the helix handedness, while z_G identifies a channel of conformations with the same value of s_G but different orientations of the side chain.

Received: January 17, 2013
Published: March 29, 2013

dx.doi.org/10.1021/ja4002508 | J. Am. Chem. Soc. 2013, 135, 5509−5512

Further details are given in sections 1.1 and 1.2 in the SI. The free energy profile reconstructed in the chirality space (Figure 1) shows two global minima that are fairly close in free energy;

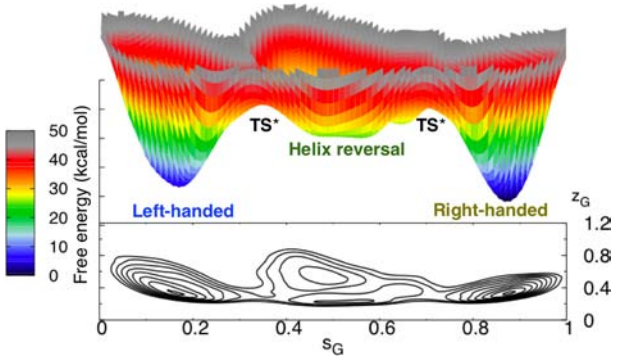

Figure 1. Free energy profile as a function of the chirality-based path-collective variables s_G and z_G. Two transition states (TS*) 38 kcal/mol higher connect the two basins.

two activation barriers of 38 kcal/mol separate them from an intermediate broad free energy basin that is 25 kcal/mol less stable than the global minima. The two global minima lie at $0 \leq s_G \leq 0.2$ and $0.8 \leq s_G \leq 1$, and the intermediate basin lies at $0.4 \leq s_G \leq 0.6$; the transition states lie at $s_G = 0.3$ and $s_G = 0.7$. It is worth noting that the free energy profile is not perfectly symmetric because the 100% right-handed and 100% left-handed helixes are diastereoisomers, as the configurations of all centers of chirality are fixed.

The main-chain chirality points to the left- and right-handedness of the free energy global minima (Figure 2). The left-handed helix is a 3_1 helix and corresponds to the values $0 \leq s_G \leq 0.2$ and $0.2 \leq z_G \leq 0.4$, while the right-handed helix is also a 3_1 helix and corresponds to the values $0.8 \leq s_G \leq 1$ and $0.2 \leq z_G \leq 0.4$. The main-chain chirality at each of the transition states shows that a helix reversal (kink) starts at the chain terminals (Figure 2). The transition states are identified by $s_G = 0.3$, $0.2 \leq z_G \leq 0.4$ and $s_G = 0.7$, $0.2 \leq z_G \leq 0.4$ for the left- and right-handed helices, respectively. These conformations are largely kinked. They further rearrange into the structures identified by $0.4 \leq s_G \leq 0.6$ and $0.2 \leq z_G \leq 0.4$, in which two helical senses coexist in the chain. A sigmoidal shape can in fact be noticed in the main-chain chirality plot of the helix reversal (Figure 2, top right).

It was proposed[14] that photoinduced rotation of the biphenyl units[15] in the side chain can trigger the helix inversion. We found that the two biphenyl dihedral angles in the side chain

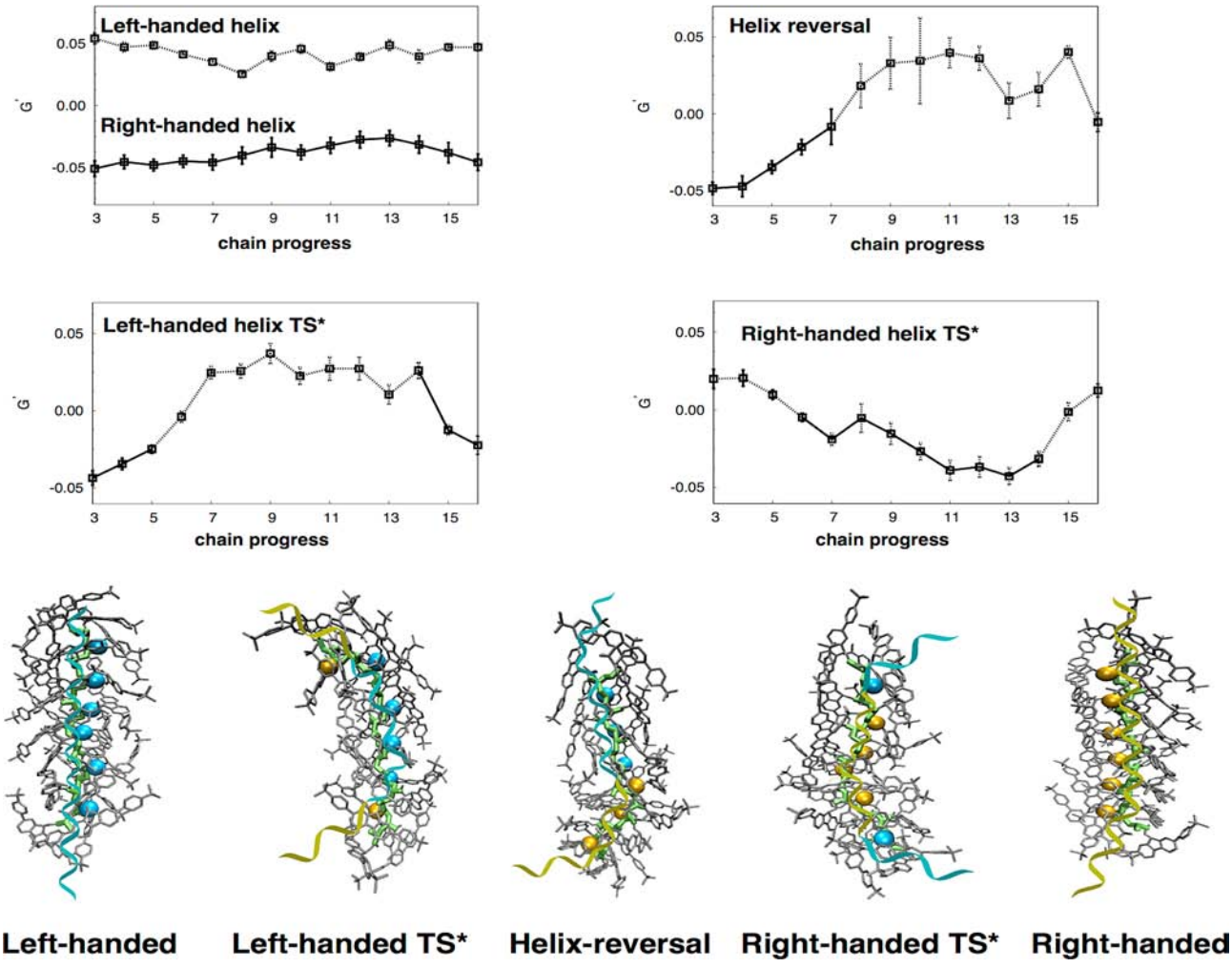

Figure 2. Main-chain chirality calculated from the different free energy basins. Left-handed (blue) and right-handed (yellow) chiralities are identified by positive and negative chirality indices, respectively.

dx.doi.org/10.1021/ja4002508 | J. Am. Chem. Soc. 2013, 135, 5509−5512

(ϕ_1 and ϕ_2) varied along the main-chain helix sense switching, where a transition between negative and positive dihedral angles was detected (Figure S3 in the SI). Moreover, at a given value of s_G, racemic values of ϕ_1 and ϕ_2 can be observed (Figure S3). This behavior is mainly detected in the central section of the polymer in the left- and right-handed global minima (Table S1 in the SI). The twisting ability of biphenyl groups has been observed in cholesteric liquid crystals,[33,34] where relatively small structural changes in biphenyl units account for specific helix inversion.[33] These results support the importance of the biphenyl rotation in the helix transition.

Through detailed analysis of typical conformations obtained in the metadynamic simulations (see section 1.3 in the SI for details and Figure S4 for structure visualization), we found that π-stacking[35] and CH$-\pi$ interactions[36] seem to have roles in the stereomutation. In the 3_1 helix global minima, the helix seems to be stabilized by the π-stacking interactions among side-chain aromatic groups. The interactions occur between residues spaced by three monomeric units, in accordance with the 3_1 helix structure. The transition states are instead featured by a close spatial arrangements between the *tert*-butyl groups and the fluorene moieties, suggesting that CH$-\pi$ interactions occur at their interface. To assess the reliability of the proposed free energy landscape, we calculated ECD spectra of the right- and left-handed conformations belonging to the global minima obtained from the simulations. We obtained ECD spectra of monomeric unit models in both the negative- and positive-twisted conformations using either TDDFT with the BH&HLYP pseudopotential[31] and the 6-31G** basis set or ZINDO.[32] The ZINDO-calculated values appeared to be red-shifted with respect to the TDDFT results, but the signs were not inverted and the overall shapes of the spectra were conserved, indicating that ZINDO is accurate enough for estimation of the ECD spectra of the chromophores studied here. Moreover, the contributions of the monomeric unit conformations were insufficient to reproduce the experimental polymer ECD spectra, in which a clear Cotton splitting was observed (Figure 3a). To extend the calculations to a longer polymer chain, we calculated the ECD spectra of hexamer models at the ZINDO level for the main clusters of right- and left-handed free energy basins (Figure 3b). The hexamer conformations were taken from the central chain sections. The two hexamers are diastereoisomers, and the single ECD spectra are therefore not perfect mirror images of each other. It is plausible that this behavior can be quenched for longer polymer chains.[14] It should be noted that the side-chain biphenyl twists in the central sections are mostly racemic (Table S1), while in the terminal sections, the side-chain biphenyl twists tend to adopt negative dihedral angles (Table S1; see Figure S7 for the ECD spectra). It is intriguing that the main-chain helicity in the central sections is independent of the side-chain twist. The calculated ECD spectrum of the left-handed helical hexamer is close to the experimental one[14] despite the higher intensity calculated from ZINDO, which is known to overestimate the rotational strength despite preserving its sign.[37] The coincidence between the calculated and experimental spectra indicates that the ECD spectral pattern mainly reflects the helical alignment of the side-chain chromophores along the helical main chain and that the conformations observed in the metadynamics simulations are credible. Also, the absolute helix sense of poly(BBPFA) synthesized using (+)-1-(2-pyrrolidinylmethyl)pyrrolidine as a chiral ligand (chirality source)[14] is left-handed.

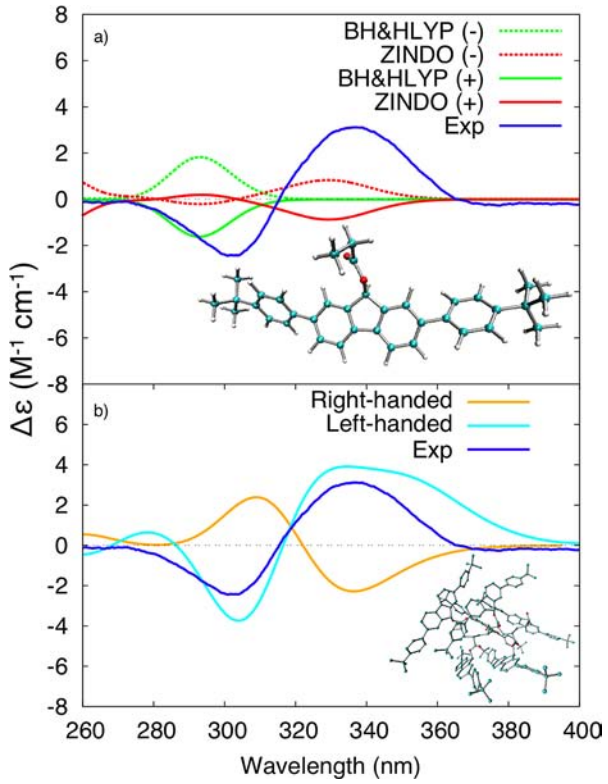

Figure 3. (a) ECD spectra calculated at the BH&HLYP[31] and ZINDO[32] levels for bis(2,7-*tert*-butylphenyl)fluorenol ethyl ester with negative (−) or positive (+) biphenyl dihedral angles. (b) ECD spectra calculated at the ZINDO[32] level for right- and left-handed hexamer central sections.

In summary, the chirality inversion of poly(BBPFA) proceeds from the left-handed 3_1 helix via multistate free energy pathways. This helix inversion is of particular interest since its racemization is not thermally accessible. This is an example of chirality inversion driven by free energy difference. The inversion is triggered by an initial rotation of biphenyl units, which is followed by a stepwise helical kink. The activation barriers of 38 kcal/mol correspond to transition states in which the main-chain chirality is inverted at the chain terminals, causing one kink in the chain. An intermediate free energy basin 25 kcal/mol higher than the global minima corresponds to right- and left-handed helical segments in a chain separated by a kink. All of the free energy basins show sections stabilized by π-stacking,[35] strongly connected to the sense of the main-chain chirality and its pitch. The transition states do not show stable π-stacking, preferring to have CH$-\pi$ interactions[36] between the *tert*-butyl groups and the fluorene units.

■ ASSOCIATED CONTENT

Ⓢ Supporting Information

Computational details, ^{1}H NMR measurements of polymer tacticity, optimized monomer coordinates, coordinates of the global minima, and rotational strengths. This material is available free of charge via the Internet at http://pubs.acs.org.

■ AUTHOR INFORMATION

Corresponding Author

tamaki.nakano@cat.hokudai.ac.jp, apietropaolo@unicz.it

dx.doi.org/10.1021/ja4002508 | *J. Am. Chem. Soc.* 2013, 135, 5509−5512

Notes

The authors declare no competing financial interest.

■ ACKNOWLEDGMENTS

PRACE Research Infrastructure resources supported part of the results achieved on the FERMI machine based in Italy. The Hokkaido University High Performance Computing System is also acknowledged for computational time. Experimental support by Dr. Takeshi Sakamoto is acknowledged. This study was supported in part by MEXT (Japan) through Grants-in-Aid 22350047 and 23655092, the Heiwa Nakajima Foundation, the Sumitomo Foundation, and the Asahi Glass Foundation.

■ REFERENCES

(1) Boersma, A. J.; Megens, R. P.; Feringa, B. L.; Roelfes, G. *Chem. Soc. Rev.* **2010**, *39*, 2083.
(2) (a) Okamoto, Y.; Nakano, T. *Chem. Rev.* **1994**, *94*, 349. (b) Nakano, T.; Okamoto, Y. *Chem. Rev.* **2001**, *101*, 4013. (c) Yashima, E.; Maeda, K.; Iida, H.; Furusho, Y.; Nagai, H. *Chem. Rev.* **2009**, *109*, 6102.
(3) Mateos-Timoneda, M. A.; Crego-Calama, M.; Reinhoudt, D. N. *Chem. Soc. Rev.* **2004**, *33*, 363.
(4) Micali, N.; Engelkamp, H.; van Rhee, P. G.; Christianen, P. C.; Monsù Scolaro, L.; Maan, J. C. *Nat. Chem.* **2012**, *12*, 201.
(5) Li, J.; Schuster, G. B.; Cheon, K.-S.; Green, M. M.; Selinger, J. V. *J. Am. Chem. Soc.* **2000**, *122*, 2603.
(6) Okamoto, Y.; Mohri, H.; Nakano, T.; Hatada, K. *J. Am. Chem. Soc.* **1989**, *111*, 5952.
(7) Ito, S.; Nozaki, K. Asymmetric Polymerization. In *Catalytic Asymmetric Synthesis*, 3rd ed.; Ojima, I., Ed.; Wiley: Hoboken, NJ, 2010.
(8) Yamamoto, T.; Yamada, T.; Nagata, Y.; Suginome, M. *J. Am. Chem. Soc.* **2010**, *132*, 7899.
(9) Ousaka, N.; Takeyama, Y.; Iida, H.; Yashima, E. *Nat. Chem.* **2011**, *3*, 856.
(10) (a) Okamoto, Y.; Ikai, T. *Chem. Soc. Rev.* **2008**, *37*, 2593. (b) Nakano, T. *J. Chromatogr., A* **2001**, *906*, 205.
(11) Ciferri, A. *Macromol. Rapid Commun.* **2002**, *23*, 511.
(12) Yu, Y.; Nakano, M.; Ikeda, T. *Nature* **2003**, *425*, 145.
(13) Ciardelli, F.; Fabbri, D.; Pieroni, O.; Fissi, A. *J. Am. Chem. Soc.* **1989**, *111*, 3470.
(14) Sakamoto, T.; Fukuda, Y.; Sato, S.; Nakano, T. *Angew. Chem., Int. Ed.* **2009**, *48*, 9308.
(15) Imamura, A.; Hoffmann, R. *J. Am. Chem. Soc.* **1968**, *90*, 5379–5385.
(16) Daura, X.; Gademann, K.; Jaun, B.; Seebach, D.; van Gunsteren, W. F.; Mark, A. E. *Angew. Chem., Int. Ed.* **1999**, *38*, 236.
(17) Csermely, P.; Palotai, R.; Nussinov, R. *Trends Biochem. Sci.* **2010**, *10*, 539.
(18) Hill, D. J.; Mio, M. J.; Prince, R. B.; Hughes, T. S.; Moore, J. S. *Chem. Rev.* **2001**, *101*, 3893.
(19) Khan, A.; Kaiser, C.; Hecht, S. *Angew. Chem., Int. Ed.* **2006**, *118*, 1912.
(20) (a) Green, M. M.; Peterson, N. C.; Sato, T.; Teramoto, A.; Cook, R.; Lifson, S. *Science* **1995**, *268*, 1860. (b) Farina, M. *Top. Stereochem.* **1987**, *17*, 1. (c) Abe, A.; Maeda, Y.; Furuya, H.; Hiromoto, A.; Kondo, T. *Polymer* **2012**, *53*, 2673. (d) Green, M. M.; Park, J.-W.; Sato, T.; Teramoto, A.; Lifson, S.; Selinger, R. L. B.; Selinger, J. V. *Angew. Chem., Int. Ed.* **1999**, *38*, 3138.
(21) Allegra, G.; Raos, G.; Vacatello, M. *Prog. Polym. Sci.* **2008**, *33*, 683.
(22) Laio, A.; Gervasio, F. L. *Rep. Prog. Phys.* **2008**, *71*, No. 126601.
(23) Wales, D. *Curr. Opin. Struct. Biol.* **2010**, *20*, 3.
(24) Osipov, M. A.; Pickup, B. T.; Dunmur, D. A. *Mol. Phys.* **1995**, *84*, 1193.
(25) Solymosi, M.; Low, R. J.; Grayson, M.; Neal, M. P. *J. Chem. Phys.* **2002**, *116*, 9875.
(26) (a) Pietropaolo, A.; Muccioli, L.; Berardi, R.; Zannoni, C. *Proteins* **2008**, *70*, 667. (b) Pietropaolo, A.; Parrinello, M. *Chirality* **2011**, *23*, 534.
(27) Pietropaolo, A.; Branduardi, D.; Bonomi, M.; Parrinello, M. *J. Comput. Chem.* **2011**, *32*, 2627.
(28) Branduardi, D.; Gervasio, F. L.; Parrinello, M. *J. Chem. Phys.* **2007**, *126*, No. 054103.
(29) Laio, A.; Parrinello, M. *Proc. Natl. Acad. Sci. U.S.A.* **2002**, *99*, 12562.
(30) Barducci, A.; Bussi, G.; Parrinello, M. *Phys. Rev. Lett.* **2008**, *100*, No. 020603.
(31) Becke, A. D. *J. Chem. Phys.* **1993**, *98*, 1372.
(32) (a) Ridley, J.; Zerner, M. *Theor. Chim. Acta* **1973**, *32*, 111. (b) Ridley, J. E.; Zerner, M. C. *J. Mol. Spectrosc.* **1974**, *50*, 457.
(33) (a) Solladie, G.; Gottarelli, G. *Tetrahedron* **1987**, *43*, 1425. (b) Katsonis, N.; Lacaze, E.; Ferrarini, A. *J. Mater. Chem.* **2012**, *22*, 7088.
(34) Gottarelli, G.; Pedulli, G. F.; Zannoni, C. *Chem. Phys.* **1982**, *64*, 143.
(35) (a) Meyer, E. A.; Castellano, R. K.; Diederich, F. *Angew. Chem., Int. Ed.* **2003**, *42*, 1210. (b) Nakano, T.; Yade, T. *J. Am. Chem. Soc.* **2003**, *125*, 15474. (c) Nakano, T. *Polym. J.* **2010**, *42*, 103.
(36) (a) Kim, E.; Paliwal, S.; Wilcox, C. S. *J. Am. Chem. Soc.* **1998**, *120*, 11192. (b) Saigo, K.; Kobayashi, Y. *Chem. Rec.* **2007**, *7*, 47.
(37) Pescitelli, G.; Narasimha, S.; Salvadori, P.; Nakanishi, K.; Berova, N.; Woody, R. W. *J. Am. Chem. Soc.* **2008**, *130*, 6170.